X-Ray Based Extensometry

Final Report on Grant NAG 3-854

12/15/87 - 12/15/88

by

E. H. Jordan and D. M. Pease
Associate Professors
Mechanical Engineering
Physics
University of Connecticut
Storrs, CT

I. Abstract

A totally new method of extensometry using an x-ray beam was proposed. The intent of the method is to provide a non contacting technique that is immune to problems associated with density variations in gaseous environments that plague optical methods. X-rays are virtually unrefractable even by solids. The new method utilizes x-ray induced x-ray fluorescence or x-ray induced optical fluorescence of targets that have melting temperatures of over 3000^{o}F. Many different variations of the basic approaches are possible. One year of an expected 3 year effort was completed when funding problems developed. In the year completed, preliminary experiments were completed which strongly suggest that the method is feasible. The x-ray induced optical fluorescence method appears to be limited to temperatures below roughly 1600^{o}F because of the overwhelming thermal optical radiation. The x-ray induced x-ray fluorescence scheme appears feasible up to very high temperatures. In this system there will be an unknown tradeoff between frequency response, cost, and accuracy. The exact tradeoff can only be estimated. It appears that for Thermo Mechanical Tests with cycle times on the order of minutes a very reasonable system may be feasible. The intended applications involve very high temperatures in both materials testing and monitoring component testing. Gas turbine engines, rocket engines, and hypersonic vehicles (NASP) all involve measurement needs that could partially be met by the proposed technology.

II. X-Ray Extensometry: Introduction

A totally new approach to extensometry was investigated which is based on x-ray induced fluorescence. The use of x-rays is motivated by a desire to overcome problems in optical noncontacting methods caused by the disruption of visible light, where the disruption is associated with air density variations inevitable in high temperature applications. X-rays are virtually unrefractable, and thus immune to problems caused by air density variations even in high pressure engine environments. The proposed method is based on knowing when a collimated x-ray beam is pointed at a fluorescing target by detecting the returning optical and/or x-rays. The beam position would be determined from the angle of collimating crystals or slits which would be monitored by the use of high accuracy optical angle encoders capable of resolving 2×10^{-6} radians. Thus, the target position can be determined and extensometry accomplished by subtracting the position of two targets. The displacement resolution of the method depends on the signal to noise ratio of the measured response.

How the Proposed Method will Work

In considering methods of using x-rays to measure strains, a large number of combinations and permutations of system characteristics have been thought of by the authors. To best explain the various options, one specific scheme will be described and other schemes will be treated as variations on the basic scheme. The basic scheme is the one deemed most promising based on preliminary experiments.

All the measurement schemes utilize a collimated x-ray beam that is directed at a target. The target is such that it will give back radiation (light or x-rays) when the incoming beam is pointed at it. In the proposed scheme, the collimated x-ray beam is scanned back and forth and the pointing angle of the incoming beam, at the time that the target responds with return radiation, is measured. Because the incoming signal is an x-ray beam, it is immune to refraction or other interfering effects. Only the timing of the response radiation is important to position determination so that refraction of the return beam will not affect the measured position as long as it does not significantly affect the timing of the measured return signal. Due to the very high speed of electromagnetic radiation, delays due to variation in index of refraction on the return beam will be nearly infinitesimal compared to other times involved. The basic scheme uses x-ray induced x-ray fluorescence, while x-ray induced optical fluorescence will be treated as a variation of the basic method. In x-ray induced x-ray fluorescence, both the generated beam and response beam are x-ray beams and thus immune to both refraction effects and interference by ambient radiation such as thermal radiation.

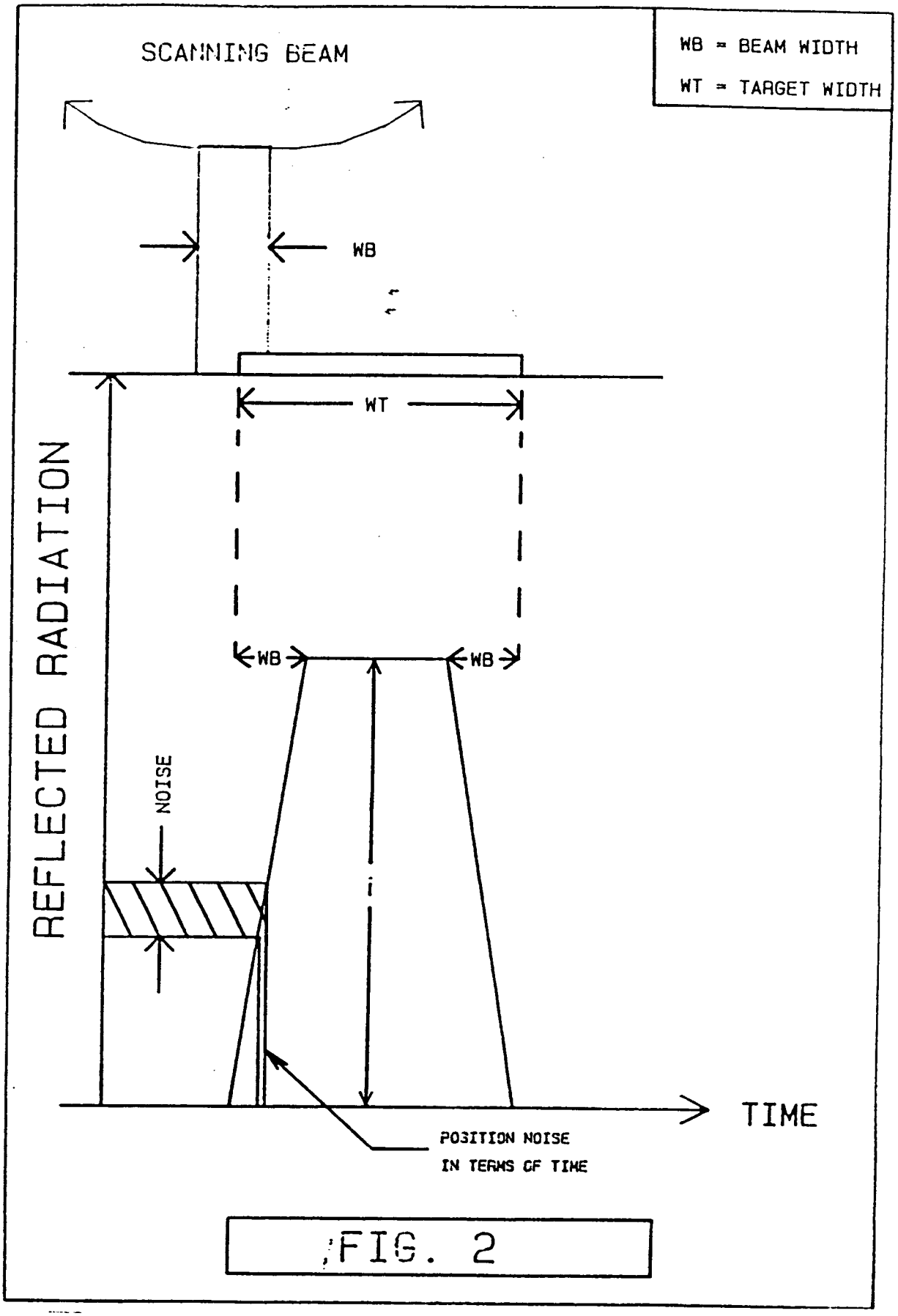
WB = BEAM WIDTH
WT = TARGET WIDTH
SCANNING BEAM
WB
WT
WB
WB
REFLECTED RADIATION
NOISE
TIME
POSITION NOISE
IN TERMS OF TIME

FIG. 2

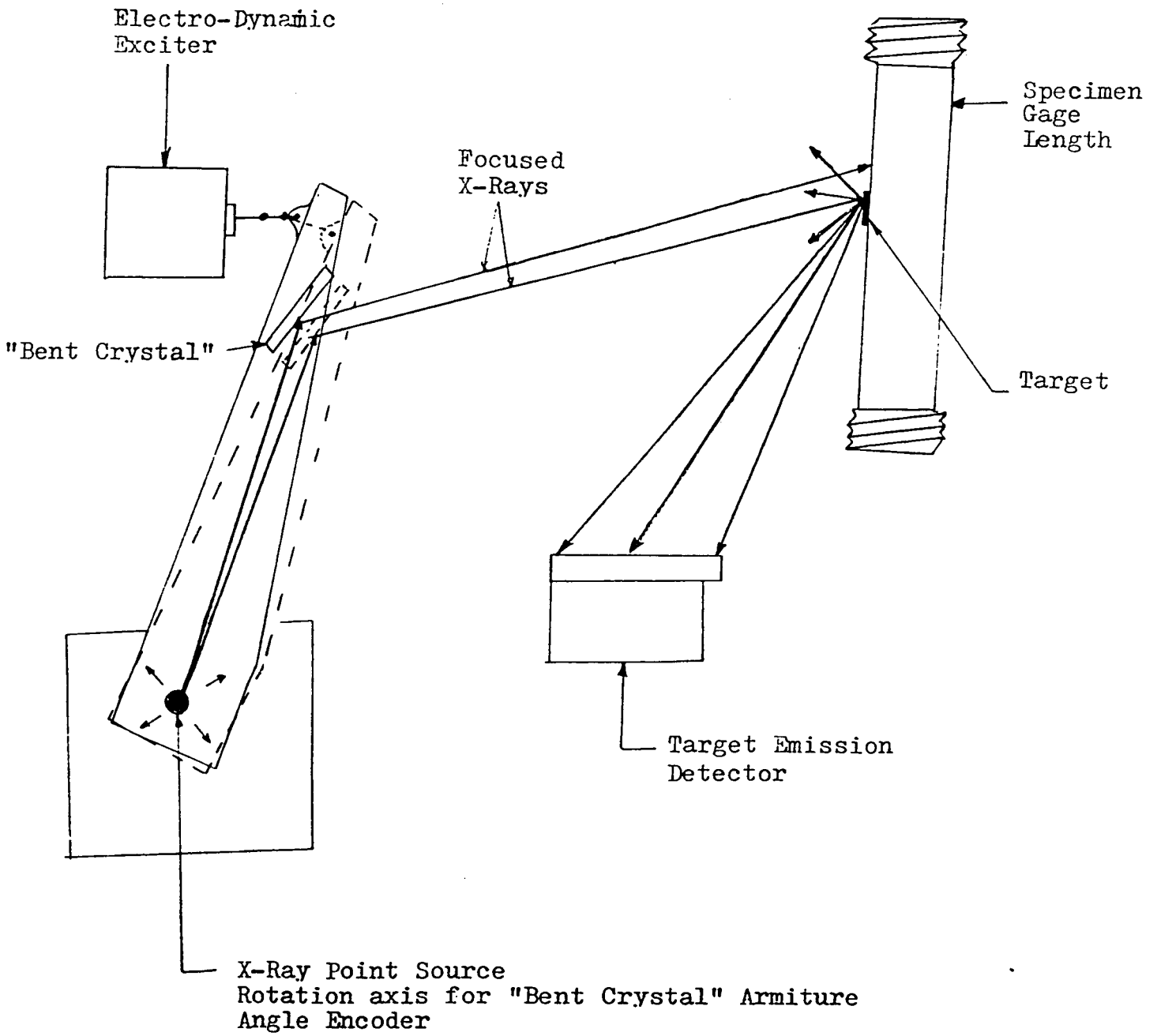
Electro-Dynamic
Exciter
Specimen
Gage
Length
Focused
X-Rays
"Bent Crystal"
Target
Target Emission
Detector
X-Ray Point Source
Rotation axis for "Bent Crystal" Armiture
Angle Encoder

Figure I

Figure 1 shows the basic configuration for displacement measurement. In this scheme, x-rays are generated at the cathode of an x-ray tube which is a line source. Some of these rays are allowed to escape and bounce off a Johannsen ground and bent bragg reflecting focusing crystal. This crystal projects the image of the filament onto the target area. Scanning the bent crystal back and forth along an arc centered at the tube filament will result in a beam that scans back and forth on the target area. The angular position of the bent crystal is measured to within 2 millionth of a radian using a Heidenhain Inc. angle encoder. The angle is recorded each time the beam exactly half overlaps the target edge, this then gives the angular position of the target four times/scan (two edges crossed on the forward scan and two on the reverse scan). If motion is in the plane and direction shown, the angle directly yields the displacement. Using two crystals mounted on the same scanner, two scanning beams can be produced and two displacements measured. Subtraction of one displacement from the other yields differential displacement needed for strain measurement. Simple sychronous detection can be used to separate the signals from the two beams using a single detector.

The basic concept of edge detection is most easily illustrated using uniform rectangular beams and targets; however, nonuniform beams and targets will behave in a completely analogous way. For nonuniform beams and targets the details of some of the relations will be changed, but the conclusions will be the same. The successful operation of the proposed scheme does not depend on beam uniformity or target uniformity; it only requires repeatability.

In the proposed setup the x-ray beam will be scanned back and forth across the target producing a fluorescence that turns on and off at the scan frequency. The resulting intensity vs. time measured by the detector is shown in fig. 2. The start of the rising part of the return radiation corresponds to the first contact of the beam with the target while peak return radiation (I in Fig. 2) corresponds to the complete overlap of the beam with the target. For the uniform beam and target shown, the percentage overlap is proportional to the percentage voltage change.This voltage represents motion of the scanned beam a distance corresponding to the beam width. The angle encoder will be read at a consistent voltage in the rising part of the beam.

For a noise free signal, this procedure would give a consistent, exact location of the beam relative to the target. In any real system there will be noise. The noise will cause nonrepeatability in detecting the edge and result in positional noise in the extensometer. This is shown in fig. 2 as the shaded area. For a well designed trigger, the width of the trigger zone will be approximately equal to the noise level. The overall spatial resolution as controlled by noise is given on the following page.

$$d = \frac{\text{noise}}{I} w$$

W = beam width
d = positional noise
I = full overlap intensity

It is clear that maximum resolution can be obtained by having a minimum width beam and maximum signal to noise ratio. As usual, these two requirements are mutually exclusive to some extent, because as the beam width decreases the integrated energy will decrease, pushing the signal level down compared to various inherent noise factors. Clearly, efforts to minimize beam width while maximizing the intensity of the reflection that occurs should be made. The success of the extensometer depends critically on the success of this effort.

In terms of signal processing, the output from the detector will be band pass filtered to minimize noise. If the x-ray beam intensity is not fully stable or if degradation of the target occurs over time, the trigger level can be normalized electronically to represent a constant beam to target overlap fraction. Synchronous detection can also be used to improve signal to noise ratios. Signal averaging may also be used to improve signal to noise ratios. Beam scanning will be accomplished by oscillating either the slit used to generate the collimated beam or oscillating the Bragg reflecting bent crystal. The range of oscillation will be on the order of a few degrees. To have backlash free motion, Bendix flexural pivots will probably be used. DB duplex angular contact bearing could be used as alternatives. To scan the beam, many schemes are possible including simple eccentric rotating drives similar to the drive system on steam trains. The exact design will have to be determined in a detailed design tradeoff study. Because of instabilities in the source, power supply and likely variations in the perfection of Bragg conditions during the scan is likely that theoretical accuracy will require normalizing the fluorescence response using knowledge of the instantaneous incoming exciter beam count rate. Fortunately, that will be possible using a thin plastic scintillator that is partially transparent to the incoming beam. The use of this pass through detector with characteristics like the fluorescence detector should allow excellent compensation for beam intensity variation.

Variation Using X-ray Induced Optical Fluorescence

X-rays will produce strong optical fluorescence for a number of high temperature materials including YAG and Yittrium oxide. These materials can be used as targets and the detection of optical fluorescence can be substituted for the x-ray fluorescence. In the proposed scheme only the timing of the fluorescence matters and hence, the refraction of the returning optical beam will not affect the position measurement. This scheme has one major advantage and one major disadvantage compared to the scheme based on x-ray induced x-ray fluorescence.

1. Light photons have energy of about 2 ev while the x-rays being used have energies around 8000 ev thus, one incoming x-ray photon can produce thousands of light photons virtually eluminating the count rate statistical noise problem present in the competing scheme.

2. Bodies at high temperature emit strong optical radiation that will compete with the optical fluorescence (see Appendix I) but will not compete with the x-ray fluorescence. The blackbody optical effects can be partially dealt with by filtering out all light except at the wave length of the strongest fluorescence peak and filtering out all DC signals from the light measuring system. Because the beam is scanned, the measurement signal is an AC signal. Detector saturation is still a consideration and this will be discussed later.

Because each scheme has its advantages, both were studied.

III. Feasibility Experiments

The performance measurement scheme just described depends upon the quantitative performance of the system elements which are the following:

1. The x-ray beam intensity and beam width.

2. The fluorescing characteristics of the target material and its tolerance of elevated temperatures.

3. The characteristic of the fluorescence response measurement system, most importantly its view factor.

4. The target attachment technology.

In general, it is desirable to have as intense and narrow a beam as possible striking a chemically stable high melting point target. The fluorescence detection system should have the largest collection as possible with low noise and large dynamic range. Target attachment should be reliable. The degree to which the conditions can be achieved determines the degree of success of the proposed system. At the outset of the project it was not known if the fluorescing efficiencies would be high enough to allow measurements to be made. The obtainable collimated x-ray beam intensities were also a matter of speculation. Accordingly, an x-ray experimental setup was constructed and feasibility experiments were run. In the following sections the test rig constructed under this grant will be described and specific experiments performed will also be presented. The data collected under this program combined with other known information will be used to discuss the feasibility of the proposed system. Additional work is advocated to demonstrate feasibility.

Description of Basic X-ray Experiments

At the beginning of the project we obtained a GE X-ray generator that was capable of supplying up to 35 KV at 15 mv to the x-ray tube. The X-ray generator and associated spectrometer were completely disassembled and moved between locations. This was accomplished, along with associated service installations, such as replacement of a defective high voltage cable, repair of a defective water pump, and several replacements of electronic components. In addition, a new safety enclosure was designed and built.

Initial operation involved the alignment of an Extended X-ray Fine Structure (EXAFS) spectrometer on the CuK $_{1,2}$ emission line. The first successful experiment was the production of visible fluorescence (red colored) from a Y_2O_3:Eu sample. The original spectrometer configuration utilized a Johannson bent and ground L_1F crystal in the (220) cut. It was suspected that increased intensity should result from a (200) cut crystal, and the spectrometer was re-aligned accordingly. The visible fluorescence, as observed through leaded acrylic plastic, was noticeably brighter. Fluorescence was then observed for various refractory materials.

In monitoring the fluorescence, the fluorescence intensity was measured both at the output of a spectrometer to measure spectral distribution and by feeding the full broadband fluorescence signal into the PMT via a light pipe. When the total PMT output was monitored by an oscilloscope, it was realized that the unfiltered, full wave rectified nature of the x-ray generator voltage produced undesirable A.C. modulation on the signal. We therefore purchased a special high voltage filter capacitor unit. After some problems with installation, this unit was installed and shown to produce a filtered output. (Perhaps it should be mentioned that our basic unit is of the old G.E. XRD6 type. One advantage of the unit is that two tubes may be operated for different set ups. We can operate with one Cu and one Mo, or two Cu tubes. A slight disadvantage is that the entire parts and service back up for scientific G.E. diffraction equipment resides in one small local company.) Further measurements of visible light fluorescence output were carried out without wavelength dispersion, by integrating the output of a light pipe leading to fluorescing targets. Results of these experiments are described below.

During the first year of our project, various positioning devices were purchased and tested, as well as a honeycomb base plate. Based on specifications and previous experience, we chose Newport positioners and motor-micrometer drives. Recently, we have determined that the jog mode of the rotary table micrometer can provide rotational increments as small as two seconds of arc, by jogging thousands of steps and watching visible rotation on the vernier index. According to the Newport engineer, these motions should be reproducible.

One possible advantage of the X-ray in, X-ray out mode over X-ray in, optical fluorescence out mode would be the competition between optical fluorescence and black body radiation from specimens at the highest temperatures anticipated. We therefore tested the x-ray in-x-ray out intensity using a Co-containing target. (CoO x-ray fluoresces well under bombardment with CuK radiation. Also, Yt0 would fluoresce well with MoK). We removed the vertical divergence soller slits from the spectrometer and produced a noticeable enhancement (x10) of the intensity up to a count rate of 1x10 CPS. Our most recent results are described below.

Finally, we have photographed the incident x-ray beam at the sharpest portion of the focusing circle, using both polaroid and high resolution film. A surprising and fortunate finding is that the beam from the bent crystal consists of two lines 6 cm long, 0.22 mm wide, 5mm apart which is quite sharp and narrow. This discovery augers well for the sensitivity of the measurement of target position. Because of the promise of fluorescence x-ray production with adequate intensity, the option of bragg diffracting marker materials has not been pursued because of the alignment difficulties relative to the fluorescence case.

Description of Estimate of the Bent Crystal Beam Intensity (I_o) Performed 2/24/89

I_0 was measured with the slits removed. The electronics were a Canberra preamp, Elscint main amplifier, Tennelc SCA, and Canberra counter/timer. The detector was operated at 1700 volts. The beam passed through the circular opening in the detector arm before reaching the detector, and was approximately aligned to go through the widest part of the opening. The intensity was measured with 9 layers of Ni foil placed in front of the detector to cut the beam down, and then scaled up accordingly. We recorded results for filament currents between 1mA and 15mA. The results listed here are for a current of 5mA. This value resulted in approximately 3.7×10^4 cts/sec with the 9 layers of foil in the beam. A plot of cts vs. filament current showed that the detection system was fairly linear at this count rate, but there actually seemed to be some "bend" in the curve even down to the lowest filament currents. We are not sure what this can be attributed to. The optical fluorescence experiment using the same electronics was very linear between 3.3×10^4 and 6.0×10^4 cts/sec, so it appears that the detector itself is nonlinear up to 10^5 cts/sec. (Also, the shape of the curve does not look like typical curves for this kind of detector in the nonlinear region.)

The total beam flux incident on the foils (within the aperature defined by the given geometry) was estimated in two ways. First, we used the fact that the ratio of the intensities through n and n+1 layers of foil is equal to exp (μx) for a single layer. Using 8 and 9 foils, we found that exp (μx) was approximately 1.65 for a single layer. The resulting estimate for I_0 is 3.3×10^6 cts/sec (for 35kV, 5mA).

We also calculated exp (μx) by using the thickness of a layer of foil measured with the gadget in the IMS metallurgy lab, and using the value of the absorption coefficient of Ni for CuK radiation from the compilation by McMaster. The value of exp (μx) obtained using a measured thickness of 13 is 1.77. The resulting estimate of I_0 is 6.2×10^6 cts/sec. The full power, full size beam count rate can be estimated by linear scaling using an average of the above two estimates as follows.

$$(4.75 \times 10^6 \text{ CPS}) \frac{15\text{mA}}{5\text{mA}} \frac{60\text{mm}}{14.2\text{mm}} = 6 \times 10^7 \text{ CPS})$$

Description of experiment to test optical fluorescence response of apparatus performed 3/1/89

The sample we measured was a 0.3 in diameter europium doped Yittrium Oxide pill. A fiber optic bundle was used with an Oriel PMT. The power supply for the PMT was a Hewlett Packard 6515, set to 1000V. The signal from the PMT was fed into the Canberra preamp, then into the Elscint amplifier, Tenelec SCA, and Canberra counter/timer. The x-ray generator was used with the constant potential assembly in place, operated at a potential of 35kV and a current of 15mA. The Lif(u.c.) Johannson bent crystal was used. The slits were taken out so that the height of the beam was 6cm. We checked that the beam was hitting the sample roughly in the center by taking a picture of the beam and measuring the relevent distances.

The fiber optic bundle was placed 21.2 mm away from the surface of the sample at an angle of 45 degrees from the plane parallel to the surface of the sample and at an angle of 30 degrees below horizontal. We also moved the bundle to 34 mm away from the sample to see whether the ratios of the squares of the distances agreed assuming an inverse square law for the intensities, and they did to within 10%.

The dark current detected with the x-ray generator turned off was 50cts/sec. We checked the linearity of the signal response by comparing the signal with a beam current of 15mA with the signal beam current of 7.5mA and found good linearity (within 1%). We checked to see whether the signal we were seeing might be due to some extraneous effect by blocking the x-rays from hitting the sample and counting, and found a count rate comparable to the dark current.

With the current set to 15mA we counted for intervals of 10 sec, 1 sec, .5 sec, and .1 sec, with 10 trials at each time interval, and compared the RMS deviation with the result predicted using poisson statistics. The average count rate we obtained was about 1.3×10^5 cts/sec. The experimental deviation for the two shortest times was the same as that predicted using poisson statistics, but was larger than predicted for the remaining cases, with a ratio of experimental-to-theoretical of 1.6 for 1 sec, and 5.5 for 10 sec counting time.

We think that this result is probably due to drift in the beam flux. The signal-to-noise ratio peaked for a counting time of .5 sec at 249.7, with values of 115.9, 222.7, and 205.3 for the .1,1, and 10 sec intervals.

Record of Optical Fluorescence Spectra

As part of the investigation, the optical fluorescence spectra of one of the candidate materials was recorded. In this experiment the bent crystal apparatus was used, but with the soller slits still in place giving approximately 10 times more narrow beam, in the vertical direction, beam (about 10 million counts/sec) than used in the other experiments. A Jarrel-Ash grating spectrometer was used and the fluorescence of Europium doped Yittrium oxide was measured and is shown in Fig. 3. The spectrum recorded at EGG Inc. using the same material, but under ultra violet stimulation which is shown in Fig. 4. Within the uncalibrated accuracy of the spectrometer used, the spectra are essentially the same. The width of the peak at 623 nm was used in estimation of the optical band pass filtering that could be used in removing competing thermal optical radiation discussed later in this report. It is apparent from Fig. 3 and 4 that filtering to less than 10 nm around the peak will dramatically reduce the light intensity available for measurement. Other materials will only be studied spectrographically if they are deemed superior to the Yittrium oxide.

Description of X-Ray Induced X-ray Fluorescence Test of Apparatus

The sample was a 1.0 in diameter disk-shaped piece of FeCo. The electronics and the settings of the x-ray generator were the same as for the optical fluorescence test. The x-ray detector was a NaI(T1) scintillation counter. The high-voltage supply was operated at 1700 V. The tube filament was placed 155mm from the center of the sample face at angles of 45 degrees from the plane of the sample surface, and 45 degrees above the horizontal. The detector surface was square-planar, 9/16 in. on a side. The solid angle subtended at the stated distance was 8.5×10^{-3} steradians.

The measured dark noise with the x-ray generator off was $\sim$75 cts/sec. The average count rate obtained with the x-ray generator operated at 35kV and 15 mA was 10^4 cts/sec. As for the optical experiment, counting times of 10,1,.5, and .1 sec were used and the RMS deviation for 10 trials was compared to poisson statistics. The experimental signal-to-noise ratios were 125.9, 103.1, 39.8, and 20.1, going from longest to shortest times. These are comparable with poisson statistics. The largest deviation was again for the 10 sec counting time, in which case the ratio between the observed and the theoretical values was 2.5.

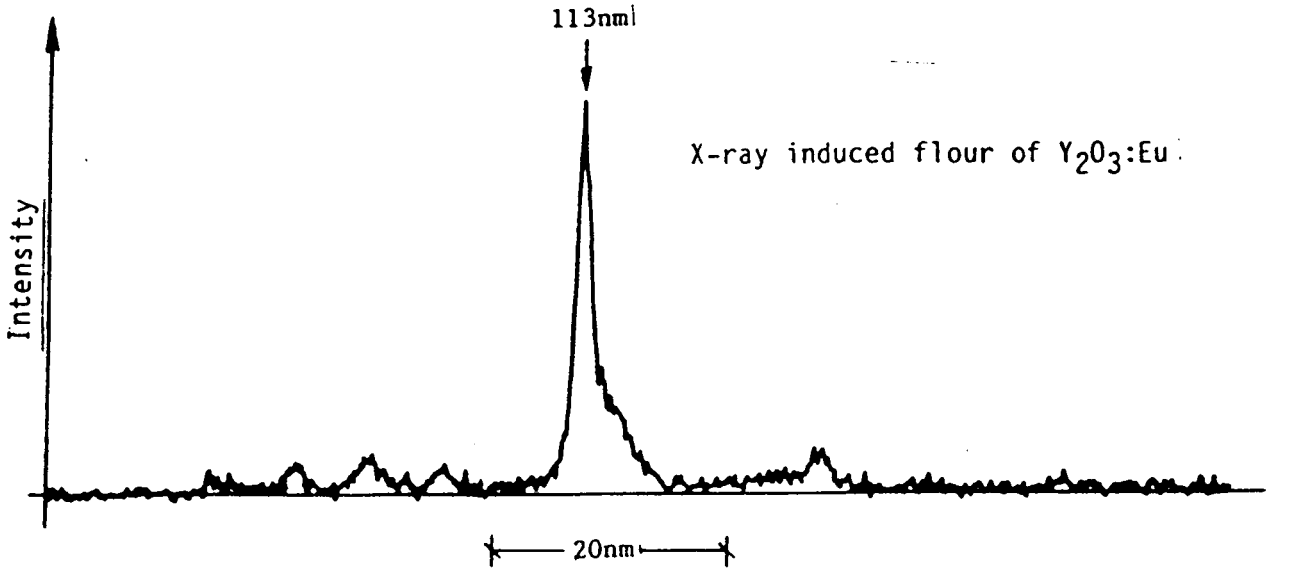

Figure 3

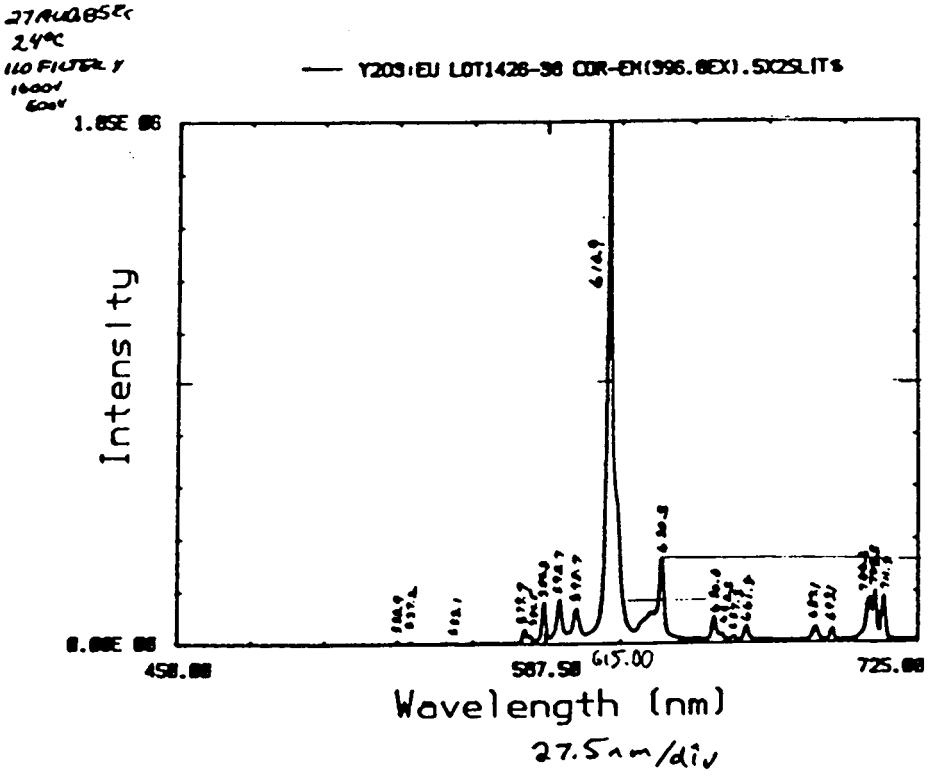

Figure 4 Ultra Violet (induced fluorescence of Y_2O_3:Eu from E.G. & G Report)

Calculation of Absolute Fluorescence at the Targets Using View Factors

Optical Fluorescence - To calculate the total fluorescence originating at the target it is necessary to account for the fact that the optical system used only collected a small fraction of the fluorescence photons. A simple approximate calculation of the view factor is easily made. Specifically, the detector bundle was 0.07 in. in diameter located .87 in from the target. A sphere 0.87 in. in diameter has an area of 9.5 square inches while the fiber optical bundle has an area of 0.0038 square inches. The bundle therefore, collects approximately 1/2400 of the possible radiation from an isotropic source. Because the target prevents fluorescence over half the sphere, the system collects roughly 1/1200th of the possible fluorescence. The count rate recorded was 130,000 cps so that at the sample the total fluorescence count rate would be 1.56 E 8 which comes from a line .31 in long. The fluorescing efficiency can be estimated as follows. The incoming beam which is 2.35 in. long has a copper k alpha x-ray count rate of 10^8. The 0.31 inch long beam striking the target has a count rate given by .31/2.35=1.3e7 CPS. Because the light photons are roughly 2 ev and the x-rays are roughly 8000 ev, 100% efficiency would yield 5.2e10 CPS. The efficiency is thus 1.56E8/5.2E10=.003=.3%. This low efficiency may be due to light doping of the sample.

X-ray fluorescence - To calculate the total x-ray fluorescence at the source, a procedure like that used above will be employed. In the fluorescence experiment, the source to detect distance was 155mm giving a sphere of area 301850 squared mm and the detector was 14.2 mm square which has an area of 204 sq mm. The detector collected about 1/1480th of an isotropic source and for the half isotropic source involved the collection of 1/740th of the photons. Using this approximate view factor and the measured count rate of 10000 cps, it would correspond to 7.4 E6 CPS at the source. The incoming beam was a 1 inch piece of the 2.36 inch beam, therefore it has a count rate given by 1/2.36 X 1E8=4.2E7 CPS. Because the energy of the fluorescing photons was nearly equal to the incident photons, the efficiency is just 7.4e6/4.2e7=.18 or 18%. Given that 1/2 the fluorescence photons go into the sample and are absorbed and the fluorescing species (cobalt) is only 50%, the efficiency would be expected to be somewhat less than 25%. The measured efficiency is quite credible considering the various approximations made. The input for the calculations that are most uncertain are the count rate in the x-ray beam in total, and exact view factor, and the exact position of the x-ray beam on the target, making the beam fraction actually hitting the target somewhat uncertain.

From both of the above calculations, large improvements in view of the factor are possible and this improvement once realized will greatly improve the potential system performance.

Potential Improvement of the Measurement Systems Elements

The performance of the measurement scheme just described depends upon the quantitative performance of the system elements which are the following:

1. The x-ray beam intensity and beam width.

2. The fluorescing characteristics of the target material and its tolerance of elevated temperatures.

3. The characteristic of the fluorescence response measurement system, most importantly its view factor.

4. The target attachment technology.

In general, it is desirable to have as intense and narrow a beam as possible striking a chemically stable high melting point target. The fluorescence detection system should have the largest collection as possible with low noise and large dynamic range. Target attachment should be reliable. The degreee to which the conditions can be achieved determines the degree of success of the proposed system. In the following section, possible improvements in the system elements will be presented. These improvements are based on existing products that have not been used yet mostly due to cost. The possible improvements combined with the data presented from this program will be shown to strongly suggest that displacement measurement is feasible.

I. X-Ray Beam Generation

The basic requirement here is to produce a narrow, high intensity X-ray beam that is sufficient to stimulate a measureable emission from the given target materials. To date, a beam with approximate dimensions of 0.2 mm by 20 mm, and with an intensity of 10 million counts per second has been achieved (this is a Cu-K alpha type beam). We view this accomplishment as very encouraging, since such intensities should make practical measurements possible. More powerful sources are available. Phillips (tm) commercially produces a compact 2200 watt X-ray source which represents a substantial increase in our current beam's power (450 watts). An increase in intensity by a factor of 4.8 can be expected by utilizing this promising piece of equipment. An additional feature of the Phillips unit is it's compact size which would allow for actual test specimen investigations performed in the elevated temperature biaxial fatigue laboratory. The cost of this source is about $18,000. At a higher price, a rotating anode source can be purchased for approximately $50,000 which has 30 times the power of the current source being used.

In addition, further intensity increases can be achieved by employing a larger "bent crystal" for X-ray beam focusing. An increase of 2-3 times the current focused count rate can be expected.

Several additional possibilities exist for large improvements in beam intensity. First, graphite has shown to have much greater reflectivity (up to three times larger) than the Li F crystals now used in our apparatus. The implication is that there is another factor of 3 in beam intensity possible. It may be possible to collect and deliver to the target a much larger (perhaps 10 times) fraction of the total x-rays coming of the tube by using a graphite barrel collector for focusing the beam or using a spaced array of Johansen bent and ground crystals with different lattice spacing so that many such crystals could be used and superimposed. The use of graphite may result in a broader line which is a potential disadvantage of graphite, but not of bent crystal arrays.

Reduction in beam width translates directly into improved displacement resolution. Elastically bent crystals are known to give much narrower beams. Estimate from vendors is that the elastically bent crystals will yield a beam up to 6 times narrower than we currently achieve.

In summary, by buying a different x-ray source count rate, improvements of up to a factor of 30 are definitely possible. Additional improvements of between 2 and 20 may be possible by different beam focusing technology.

Combining the two above changes, an intensity increase of approximately 15 times would be achieved, without the expensive rotating anode source and improvements of several hundred times are possible with the rotating anode source. The proposed experiments will be done using the existing source and results can be extrapolated to be achievable with these source improvements. Only the larger bent crystal enchancement will be implemented in the current program.

As an alternative to using a bent crystal, the diverging beam can be collimated by using a long narrow slit that only allows radiation leaving at the desired angle to pass through. A slit which would give a 1 degree divergence has been tested and found to have a count rate similar to, but less than the bent crystal. More importantly the beam width was much larger than the bent crystal (more than 10 times). The enhancements discussed above involving the power of the x-ray source would apply to this source, but these involving other improvements would not. In summary, this beam generation method appears less desirable than using the bent crystal, but still might be of interest if a situation arises where the bent crystal could not be used. Such a situation could arise if a very large standoff distance were needed.

II. Target types

X-Ray Fluorescing

For x-ray induced x-ray fluorescence, two fluorescing materials are being considered at present, the first of which has actually been tested. An experiment has been completed in which iron cobalt is fluoresced by copper K-alpha radiation. The existing bent crystal setup is designed to utilize copper K-alpha radiation.

In this experiment cobalt oxide was fluorescenced using the 10 million counts/second copper K-alpha beam. With a .25 square inch detector 4 inches from the cobalt oxide target, 10^4 counts/sec were recorded. In the proposed experiment, the 20" x 20" detector described in the next section will be used. The detected count rate is expected to be more than half a million (Counts/sec) which is a large enough count rate to make a good displacement measuring setup.

A second material being considered is yittrium oxide fluoresced with more energetic molybdenum copper K-alpha radiation. This combination is expected to be a high efficiency fluorescing pair similar to the first. Fluorescence can be forecast based on absorption edge energies compared to source beam energy. Both cobalt oxide and yittrium oxide melt at over 4000^{o} F and would make very suitable high temperature target materials. The system using yittrium oxide would be advantageous in high density air because it penetrates air 8 times better than copper k-alpha.

In both of these systems it is desirable to detect the highest obtainable fluorescence count rate. This can be done by having a very large detector or a very powerful x-ray beam. Fortunately, an affordable large detector is commercially available.

Optical Fluorescing

For x-ray induced optical fluorescene, candidate materials are not simple to identify. Fortunately, the investigators are in close contact with Mr. Borella of E.G. and G. Inc. Mr. Borella and his organization are working very actively in the area of fluorescence thermometry and are continuosly collecting different high temperature fluorescing materials. To date, Mr. Borella of EG&G Inc. has supplied us with 5 different candidate fluorescing materials as follows

a) Y_2O_3: Eu powder
b) $Mg_4(F)GeO$: Mn powder
c) $Y_3Al_5O_{12}$: Tb powder (YAG)
d) $Y_3AL_5O_{12}$: Dy chip (YAG)
e) $Y3AL_5O_{12}$: Ce powder (YAG)
f) $La2O_2S$: Eu
g) Y_2O_2S: Tb

EG&G. Inc. data on the properties of these materials is available to us. We have tested only the first of these so far. Currently, fluorescing materials with high temperature stability are being investigated by DOD for display and electro optical applications and Japanese companies are rumoured to be planning to get into the business of producing these materials. It is therefore, to be expected that increasingly good materials at lower and lower prices will continue to appear.

III. Fluorescence Detection Methods

For purposes of x-ray fluorescence detection, Bicron Inc. sells plastic scintillation counters that are available in sizes up to several feet by several feet. As an example, a 20 x 20 inch collector 8 inches away would have recorded a fluorescing count rate on the order of 1,000,000 counts/sec in the above mentioned experiments. To protect the plastic detector form thermal radiation, in order that it can be brought as close as possible to the target, thin heat shields of metal could be used, which would attenuate the x-rays. For example, several layers of aluminum foil or nickel foil could be used. It would be possible to air cool these heat shields. It may also be possible to use metal coated high temperature plastic such as ICI inc. peek, plated with nickel. In any case, heat shields are clearly possible and should allow reasonably close placement of the detectors so as to bring the recordable count rates to levels which should allow good measurements of displacement.

For purposes of optical fluorescence detection, photomultiplier tubes are very sensitive devices and available with a wide variety of spectral responses. Accordingly, they are suitable for use in this project. To make good use of the existing tubes, optical band pass filters will be purchased to block stray light. The current system uses a .2 inch dia light pipe about 1.5 inches from the target which gives a collection efficiency of about 0.001. By using a 35 mm camera lens and macro filters, it will be possible to improve the collection efficiency to approximately 0.02 which will give over a factor of 20 improvement in the collection ratio, and by imaging the target on the light pipe, the thermal radiation from other than the target area can be eliminated. At higher temperatures the cameral will have to be moved further away reducing the collection ratio, perhaps back to about 0.003.

IV Beam Scanning Methods

In order for displacements to be measured, it is necessary to scan the beam back and forth. The proposed method of accomplishing this involves rotation about the x-ray tube filament centerline. The x-ray beams used originate from a filament and are therefore line sources. The methods described in previous sections may be used to generate a collimated beam. A Johannsen ground and bent crystal may be used or the line source may be collimated by passing through a long narrow slit. For both of these methods the beam collimating device needs to rotate around the center of the filament to maintain maximum beam strength. The crystal needs to maintain a constant incident angle to satisfy the bragg condition and the slit needs to keep the filament in the line of sight from the target through the slit back to the filament. Beam scanning can be accomplished by mounting the slit or bent crystal on an arm pivoted around the filament center. Fortunately, because of the x-ray tube geometry, it is physically possible to mount a bearing set under the tube directly under the center of the filament. For low frequency simulation, the arm will be mounted on an existing DC motor driven rotary stage.

For the dynamic set up, the designed visualization involves DB duplex bearing holding a shaft free of all axial or radial clearance connected to a spring loaded excited to torsional resonance by a rotating eccentric mass. See Fig. 1.

V Target Attachment

A number of target attachment methods may be possible. Flame spraying, sputtering, Ion implanting, or mechanical attachment are all possible and some cracking, as long as not accompanied by spalling, would be tolerable. Mechanical attachment is challenging because of the inevitable mismatch of thermal expansion coefficients. The simplest scheme involves simply hanging the target on a "high temperature string". Such a scheme has been used successfully in attaching white markers to metal samples at 1800°F in metals testing. Candidate high temperature strings include platinum - rhodium thermocouple wire, Nextel fibers, and Nicalon fibers. An additional scheme involves attaching a fiber matt or batting to the specimen and attaching the target to the other side of the batting. This will allow the fiber batt to accommodate any expansion mismatch. Possible adhesives include high temperature glasses that show excellent properties in different temperature ranges and form the basis of the increasingly important ceramic glass composites. Additional adhesive schemes could be conceived of using commercial adhesives. Another scheme could involve the addition of tabs of material from which the sample is made upon which the target could be rested or trapped. In the case of ceramic glass composites such tabs could be made from glass and put on by the dyes used in hot pressing the sample.

Of the various attachment schemes the high temperature string concept has already been used successfully and should work up to the limit temperature of the fiber used which for thermocouple wire, is 1600°C, for nextel is 1400°C, and for Zirconia is 2200°C. Since these materials are among the primary candidates for the specimen material, the method should be good to as high a temperature as the sample.

For specimen testing, NBS has developed a gravity induced friction method that involves a device looking like a high temperature clothes pin. This proven technology can be used as a backup method.

In summary, a wide variety of methods are possible. For the purpose of this grant, the method that is intended is to tie the target on the platinum wire. This method which we have used successfully at lower temperatures should work well and is simple and allows temperatures up to 3000°F.

All line of sight measurement methods are affected by rigid body motion and most especially rotations. Methods subjected to essentially the same effects include the laser based system of Optra Inc., the Servo Camera of Optron Inc., the shadow method of Zygo Inc., and the proposed method.

For material test applications, these effects appear to be unimportant. Good results have been obtained by others using both the Optron system and the Zygo system. These systems would however, be expected to have difficulties in the presence of strongly refracting hot gas layers. For other than material test situations, errors may occur and these are discussed in Appendix II. These errors can be eliminated if all three components of displacement are measured. The proposed method has the potential for making such three D displacement measurements and the Mathematics for the required corrections is contained in the Appendix.

Conclusions

Experiments have been done that strongly suggest that x-ray extensometry is possible. Prior to this program, it was not known what collimated beam characteristics were possible with the available apparatus. The current beam has 10E8 CPS and a width of .22 mm. This beam can be enhanced by up to a factor of 100 in intensity and up to a factor of five on narrowness using existing, but more expensive technology. Our preliminary results indicate that with increases in view factor using readily available and in expensive large area detector count/rates on the order of 10E6 should be achieved with the current beam generation scheme. Because of the fact that the optical scheme yields a similar count rate as the x-ray scheme at the detector, and that this method is limited to lower temperatures by interfering thermal radiation, the x-ray induced x-ray fluorescence scheme appears the most promising.

To a first order, improved collection in combination with the improved beam should yield a displacement resolution of 2E-4mm at 1 hz where the S/N ratio is assumed to be equal to the square root of the count rate as would be expected from Poission statistics. To actually achieve this theoretical resolution will require the solution of a number of technical problems. At this time, two of the problems are expected to be the most challenging. The first is developing a beam scanning mechanism that is percise enough to maintain bragg conditions throughout the scan. The second is developing a convenient target attachment method. The resulting method will have the same limitations with respect to rigid body effects as other line of sight methods. If these problems are overcome, a method for use in very hostile environment will become available. Because of the increasing interest in very high temperature materials and the need for data from rocket and jet engines further development of this method is recommended.

APPENDIX I

Thermal Radiation Effects on Optical Fluorescence Measurements

As temperature is increased, the amount of optical thermal radiation rapidly increases. This thermal radiation will tend to saturate the detector used for detecting fluorescence at some point. Any good system design will employ band pass optical filtering that only let through wave lengths near the peak fluorescence wave length. To understand the quantitative aspects of this, the optical fluorescence is estimated to be roughly 10 watts/mm. The thermal black body radiation in a given wave length band can readily be calculated. Below is a table where thermal radiation is calculated in various 20 nm bands and can compare to the fluorescence radiation at two temperatures. 20 nm was chosen as it represents the approximate width of the fluorescence peak of yittra oxide for which we have a spectral trace.

Body Temperature	Radiation watts in a band from .42nm-44nm	Radiation watts in a band from .52nm-.54nm	Radiation watts in a band from .62 to 64mm
1560°F	6.15 x 10-11	5.8 x 10-9	1.1 x 10-7watt/mm
3000°F	1.4 x 10-5	1.3 x 10-4	5.2 x 10-4

As can be seen, the thermal radiation is comparable to the fluorescence at 1600°F and overwhelms it at 3000°F. Signal processing can be used to block the DC thermal radiation, however, the photo multiplier gain must be reduced to avoid saturation. It is worth noting that lock-in amplifiers can easily extract signals from sources with a S/N ratio of 10-6. However, in light of how the x-ray induced x-ray fluorescence avoids this entire problem, it would appear that x-ray induced optical fluorescence is best limited to temperatures below 1600°F.

Appendix I

Determination of Strains from Displacements with Small Strains and Large Rotations

A number of measurement methods allow the measurement of differential displacements optically such as the shadow methods used by Zygo Inc., servo imaging methods of Optron Inc., speckele based method used by Optra Inc., simple grid methods as well as a beam target overlap method and a beam pointing method proposed recently by Jordan. In all of these methods the potential effects of rigid body motions must be considered. Here we will consider two questions. First, what is the nature of the error resulting from unrecognized rigid body rotations? Second, if enough displacement information is available, how might the strains be correctly calculated from the displacements? In this discussion of these questions, two assumptions will be made as follows:

1. The rotations may be large, but the strain is small compared to one such that the strain squared is small compared to the strain, and sine of the angle change associated with shear is approximately equal to the angle itself.

2. The displacement is measured at two points that are sufficiently close together such that the displacement gradient is well represented by difference quantities. This assumption is used in most strain measurements.

In discussing these questions, advantage will be taken of the properties of the Lagrangian strain tensor in its general form appropriate for finite strains. This strain measure will turn out to have very useful characteristics for handling rigid body rotations.

In the following, it will be shown that the Lagrangian strain tensor defined in terms of displacement derivatives, is useful in determining infinitesimal strains in the presence of large rotations. Following that, several different cases in which less than full displacement information is available will be examined. Errors resulting from rigid body rotations will be discussed. The basic information concerning strain measures and their interpretation is available in most continuum mechanics text books. The facts for the following discussion and notation was taken primarily from ref. 1.

Consider a particle in a deformable body whose position in the undeformed state is given by position vector X and whose position in the deformed body is given by position vector x. If the deformation field were fully known, then the following relations could be written

$$x = x(X,t) \text{ or } x_i = x_i(X_1,X_2,X_3,t)$$

and inversely by

$$X = X(x,t) \text{ or } X_i = X_i(x_1,x_2,x_3,t)$$

The displacement components will be defined as follows:

$$x_i = X_i + u_i$$

with displacement components

$$u_i = u_i(X_1, X_2, X_3, t)$$

The Lagrangian strain measure will be defined as giving the change in the squared length of the differential position vector dX as follows:

$$(ds)^2 - (dS)^2 = 2dX \cdot E \cdot dX$$

$$(ds)^2 - (dS)^2 = 2dX_i E_{ij} dX_j$$

In the proposed strain measurement method, displacements are determined. With sufficient information about the displacements strains may be calculated. The following strain displacement relations (1) apply

$$E_{ij} = 1/2 \left(\frac{\partial u_i}{\partial X_j} + \frac{\partial u_j}{\partial X_i} + \frac{\partial u_k}{\partial X_i} \frac{\partial u_k}{\partial X_j} \right)$$

for the 22 and 12 component for example:

$$E_{11} = \frac{\partial u_1}{\partial X_1} + \frac{1}{2} \left[\left(\frac{\partial u_1}{\partial X_1} \right)^2 + \left(\frac{\partial u_2}{\partial X_1} \right)^2 + \left(\frac{\partial u_3}{\partial X_1} \right)^2 \right]$$

$$E_{12} = \frac{1}{2} \left(\frac{\partial u_1}{\partial X_2} + \frac{\partial u_2}{\partial X_1} \right) + \frac{1}{2} \left(\frac{\partial u_1}{\partial X_1} \frac{\partial u_1}{\partial X_2} + \frac{\partial u_2}{\partial X_1} \frac{\partial u_2}{\partial X_2} + \frac{\partial u_3}{\partial X_1} \frac{\partial u_3}{\partial X_2} \right)$$

What now remains is to show how to determine the infinitesimal strain in the presence of finite rotations from displacement components using the above strain measure. It is clear that for displacement derivatives that are small compared to 1, all the quadratic terms in the above equations may be neglected and the strain displacement relations are then identical to the infinitesimal ones. Here, however, we wish to consider the case of finite rotations with infinitesimal extensions. Engineering extensional strain is the change in length divided by the original length. For the differential quantities being considered, engineering strain would be (ds-dS) /dS which is often referred to as the unit extension and can be shown to be related to the Lagrangian strain measure (1) as follows:

$$\frac{ds-dS}{dS} = 1 + 2 E_{11} - 1$$

whence

$$E_{11} = E_{(1)} + 1/2 \, E^2_{(11)}$$

By assumption 1 the right hand term in the above equation is negligible and the diagonal terms in the Lagrangian strain tensor are equal to the infinitesimal engineering strain even for finite rotations so long as the extension ratio is infinitesimal.

Engineering shear strain is one half the angle change between two edges of a rectangular element which are initally parallel to the coordinate axes. It can be shown (1) that angle between two axes for example, the 1 and 2 axis after deformation will be:

$$\cos \Theta_{12} = \frac{2E_{12}}{\sqrt{(1 + 2E_{11})(1 + 2E_{22})}}$$

which for small extensionable strains becomes:

$$\cos \Theta_{12} = 2E_{12}$$

The shear strain as defined as 1/2 the angle change would then be as follows:

$$\pi/2 - \Theta_{12} \approx \sin (\pi/2 - \Theta_{12}) = \cos \Theta_{12} \approx 2E_{12}$$

For small angle change E_{12} = 1/2 the angle change is the usual small strain shear tensor component.

By a virtue of the shear being small in the sense that sin of the angle change is approximately equal to the angle change, the component of the Lagrangian strain measure is equal to the one half engineering shear strain. This equally requires only small angle changes and still holds for large rigid body rotations.

In summary, the rectangular cartesian form of the chosen strain measure has components which are equal to the infinitesimal strain measure most often used in engineering provided that the extensional strain and shear strain are small. This interpretation of the components of the strain measure hold even for finite rigid body rotations. In exactly what sense the term small strains is to be interpreted is clear from the above presentation. Accordingly, it is proposed that the strain displacement relations given in equation 4 be used to calculate strains from measured displacements in the presence of rigid body rotations.

Errors in Determining Strains from Unrecognized Rigid Body Rotations

Case 1 One component of displacement measured at two points

Traditional extensometry involves measuring one displacement component at two places and computing the strain as the differential displacement divided by the gage length. Figure 1 shows a gage section which is parallel to the y axis and over that gage length experiences a uniform strain E_y.

In the case being considered, rigid body rotations have occured such that the gage section which first made angles of the x,y,z axes of 90,0,90 now make angles of Θ_x Θ_y Θ_z. From the figure, the following differential displacements and associated directives can be written:

$$\frac{\Delta v_1}{\Delta y} = (1 + \varepsilon_y) \cos\Theta_x \qquad \frac{\Delta v_2}{\Delta y} = (1 + \varepsilon_y) \cos\Theta_y - 1$$

$$\frac{\Delta v_3}{\Delta y} = (1 + \varepsilon_y) \cos\Theta_{z_1}$$

Substitution of these values into equation yields the Lagrangian strain component E exactly equal to the extensional strain ε_y. In the case being considered, only the y component of displacement is measured and the experimentalist is forced to assume that dv/dy equals the extensional strain. This results in the following expression for the measured strain:

$$\varepsilon_y = 1 - (1 + \varepsilon_y) \cos\Theta = 1 - \cos\Theta_y + \cos\Theta_y \varepsilon_y$$

Fig 2 shows the error in strain as function of an angle of rigid body rotation and applied strain resulting from assuming the above expression, was equal to the extensional strain. Rigid body rotations as small as 2^o produce errors larger than 5% for $\varepsilon_y = 0.01$.

Case II Three Components of Displacement known at two points

In equation 4,5 it can be seen that the extensional strain associated with the 2 direction only involves derivatives of the displacements with respect to X. This means that this component of strain can be determined correctly from measuring the three displacements at two points. The in plane shear cannot be determined without determining all the displacements at three or more points.

Case III Three components of Displacement known at three neighboring points not in a straight line

In equation 4,5 it can be seen that the in plane shear strain expression only variation of the displacements in the in plane directions. Case III allows the determination of both the shear and extensional strain exactly.

References

1. Malvern L.E., "Introduction to the Mechanics of a Continuous Medium", Prentice-Hall, Inc., Englewood Cliffs, New Jersey, 1969.

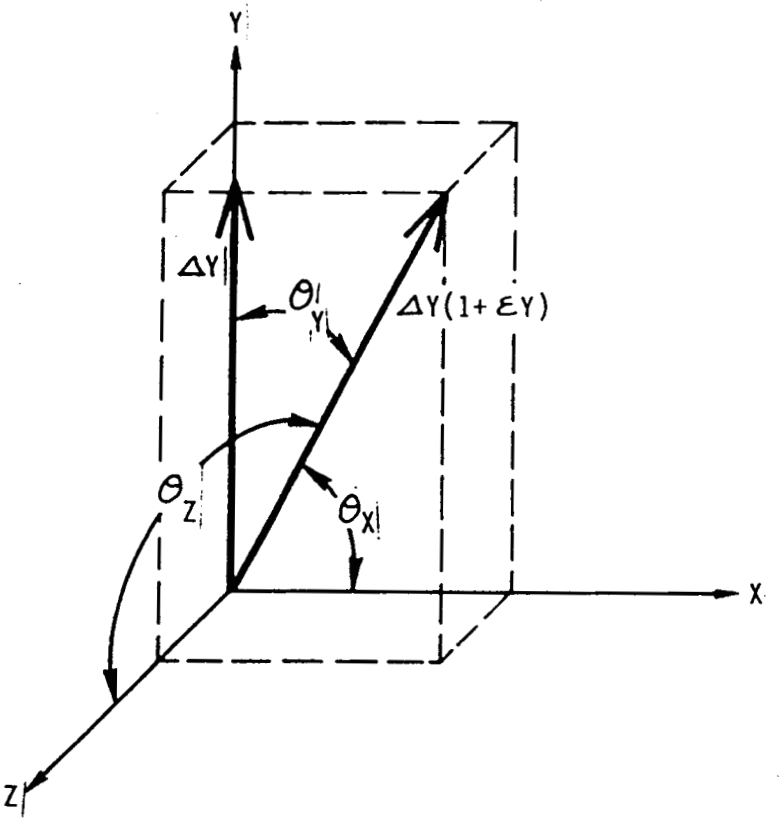

Figure 1 Effect of rotation on apparent strain on gage length Δ_y